Verification of an Optimized Condition for Low Residual Stress Employed Water-Shower Cooling during Welding in Austenitic Stainless Steel Plates

Nobuyoshi Yanagida, Material Research Laboratory, Hitachi, Ltd.
Kunio Enomoto, Hitachi Engineering Consulting Co. Ltd.
Hideya Anzai, Nuclear System Division, Hitachi, Ltd.

30th MPA-Seminar in conjunction with the 9th German-Japanese Seminar
Stuttgart, October 6 and 7, 2004

Abstract

To reduce tensile residual stress in a welded region, we have developed a new cooling method that uses a water-shower behind the welding torch. When this method is applied to the welding of austenitic stainless steel, the welding and cooling conditions mainly determine how much the residual stress can be reduced. To optimize these conditions, we first used a robust design method to determine the effects of the preheating temperature, the heat input quantity, and the water-shower area on the residual stress, and found that, to decrease the tensile residual stress, the preheating temperature should be high, the heat input low, and the water-shower area large. To confirm the effectiveness of these optimized conditions, the residual stresses under optimized or non-optimized conditions were measured experimentally. It was found that the residual stresses were tensile under the non-optimized conditions, but compressive under the optimized ones. These measurements agree well with the 3D-FEM analyses. It can therefore be concluded that the optimized conditions are valid and appropriate for reducing residual stress in an austenitic stainless-steel weld.

1. Introduction

Stress corrosion cracking (SCC) of austenitic stainless-steel welds in power-generating plants has been one of the main concerns requiring mitigation. Reducing high tensile residual stress can control the onset of SCC.

Controlling the temperature distribution in welded structures is one way to reduce tensile residual stress (Ueda, 1986; Ueda, 1983; Rybicki, 1982; Shimizu, 1987; Sakata, 1988). An example is heat sink welding (Ueda, 1986; Ueda, 1983), which was developed to reduce the tensile residual stress on the surface opposite to the last welding pass. The last pass on the surface of the structure is made while the side opposite the welded surface is water cooled. As a result, the temperature of the last-pass welded surface is higher than that of the opposite-side surface. These thermal and welding processes reduce the tensile residual stress on the surface of the opposite side. This technique has been applied to reduce the tensile residual stresses on the inside of a butt-welded pipe joint.

In the case that the last-pass side is exposed to a corrosive environment, it is important to reduce the tensile residual stress on that side. Underwater welding (White, 1997) is an example in which tensile residual stress on the surface of the last pass welded side is reduced. In this welding process, the surrounding water rapidly cools the area heated by the torch. The temperature at the outside surface of the welded region thus becomes lower than that of the inside surface of the structure. These thermal and welding processes reduce the tensile residual stress on the surface of the last-pass welded side of the structure.

On the other hand, there have been few studies on ways to reduce tensile stress on the surface of a structure during the last pass when the welding is done in air. Most welded structures are manufactured under ambient conditions; therefore, a technique that reduces tensile stress during the last pass on the welded side in air is particularly important. Against this background, we developed a welding method that reduces the tensile residual stresses on the surface of the last welded layer in air. To evaluate the method, we analytically and experimentally examined the residual-stress distribution of an austenitic stainless-steel plate welded and then cooled rapidly. The plate was bead welded. After the welding, the whole surface of the welded side was cooled by a water-shower. This idea was verified by experiment; it was found that rapid water-shower cooling of the plate decreases the residual stress. However, the effects of welding conditions on residual stress reduction, such as torch travel speed, the number of welding passes, and interpass temperature, were not determined, nor were the effects of cooling conditions, such as the area of the water-shower, the distance between the torch and water-shower, and the shower rate. Knowing the effects of these factors on residual stress reduction will be useful.

In this study, welding residual stresses were analyzed for various welding and cooling conditions using a two-dimensional finite-element method (2D-FEM). To determine the effects of various conditions on residual welding stress, we applied a robust-design technique for evaluation of the S/N ratio and sensitivity. The effects of each condition on tensile residual stress were estimated. The optimized conditions were determined considering these effects. The mechanism of tensile residual stress reduction was also examined using a three-dimensional finite-element method (3D-FEM). The effects of the preheating temperature and rapid water cooling on residual stress distributions were verified through these analyses and experiments.

2. Mechanism to reduce tensile residual stress by water-shower cooling

Figure 1 is a schematic of the new welding method. Rapid cooling is done using a water-shower behind the torch after the last pass. The objective of the rapid cooling is to control the onset of SCC. Therefore, the residual stress on the surface of the plate should be made compressive on the welded surface. Thus, it is important to generate compressive residual stress in the whole region around the welding bead by adjusting the parameter values.

Figure 2 shows the temperature and stress distributions during two welding processes. In the first one (top of Fig. 2), the top surface of a plate is heated for a short time and then cooled. As the surface is heated, thermal expansion occurs. This expansion is restricted by the bulk of the plate. Compressive stress, followed by compressive yield, thus occurs around the heated surface. Compressive plastic strain therefore remains on the surface of the plate after the heating process. And after moderate cooling, this compressive plastic strain generates tensile residual stress.

In contrast, in the second process (bottom of Fig. 2), after the surface of one side of the plate is heated for a short time, it is cooled by a water-shower. The temperature around the surface of the plate decreases rapidly when the water-shower is applied, but the temperature inside the plate remains high. During cooling, tensile stress occurs only on the surface of the plate, so tensile plastic strain remains near the surface of the plate. After moderate cooling, the tensile plastic strain generates compressive residual stress.

3. Determination of the optimized conditions

3.1 Problem formulation

A parameter that can be set to any value by the operator is a controllable parameter. Controllable parameters in this welding method are shown in Figure 3. They are (A) the number of welding passes at the last layer, (B) the interpass temperature, (C) heat input, (D) torch 'travel speed, (E) the distance between the torch and cooling area, (F) the width of the cooling region, (G) the depth of the cooling region, and (H) the water-shower rate. Table 1 shows the controllable parameters and their levels. The standard value of each parameter is the second level. The maximum or minimum value is the first or third level.

A variable that should be monitored for optimum performance is a signal factor. Here, residual stress is the signal factor. A parameter that affects the signal factor and cannot be controlled by the operator is an error factor. Shower-water temperature, the position along a welding bead, and directions of stresses are error factors. In this study, shower-water temperatures were 0 and 40 °C. Positions were welding-start, -steady, and termination regions. For each position, the longitudinal and transverse stresses on the welding bead, fusion line, and heat-affected zone (HAZ) were estimated.

3.2 Data collection / simulation

In the optimum process, whose conditions comprise combinations of many controllable parameters, it is unreasonable to examine all combinations of parameters. To estimate the effects of the controllable parameters on signal factors, we need a convenient experimental design. An L18 orthogonal array is often used to evaluate eight sets of controllable parameters. Table 2 shows the combinations of controllable parameters. The effects of controllable parameters on signal factors can be estimated by 18 sets of experiments. In the experimental conditions shown in Table 2, Condition 1 indicates that the signal factor should be measured in the case of A1, B1, C1, D1, E1, F1, G1, and H1, where the letters are the parameters and the numerals the level: A1 indicates the first level of control parameter A.

To determine the residual stress distribution for the conditions in Table 2, we did 2D-FEM analyses. A transient heat transfer analysis was done first to calculate temperature distributions during the welding and cooling processes. Then a thermal

elasto-plastic analysis was performed based on the temperature distributions calculated in the heat transfer analysis.

FEM analyses were performed using a two-dimensional model. Three cases had to be analyzed for each condition in Table 2 to determine residual stresses in the welding-start, welding-steady, and welding-stop regions. Figure 4 shows cross sections of these positions.

A thermal elasto-plastic analysis was done using the history of temperature distribution determined by the transient heat transfer analysis. The stress at the moment when the temperature finally reached room temperature is the residual stress. The evaluation positions of the residual stress were the center of the bead, a fusion line, and the HAZ. Residual stresses were evaluated in longitudinal and transverse directions. Contour lines of residual stress in analytical conditions No. 1 and No. 16 are shown in Figures 5 and 6 as examples of the FEM results. The residual stresses in Figure 5 are not compressive enough on the surface of the plate. On the other hand, stresses in Figure 6 are compressive enough.

3.3 Factor effects analysis

It is difficult to determine the effects of each condition shown in Table 2 on the residual stresses calculated by the FEM. To determine the effects of each condition on residual stresses, we did a data analysis using the nominal-the-best S/N ratio. Figure 7 shows the flow of data analysis. The S/N ratio and each sensitivity were calculated for each level of the controllable parameters. A factor-effect map was made and is shown in Figure 8.

The level that maximizes the S/N ratio in a controllable parameter minimizes the variance of the residual stresses. The level that maximizes the sensitivity in each controllable parameter maximizes the absolute value of the compressive residual stresses. To determine the optimized conditions, first, the level that maximizes the S/N ratio and sensitivity was determined. Conditions A2, B3, F1, G3, and H2 were set as the optimized ones. In the case that the level maximizes the S/N ratio but not the sensitivity, the level that maximizes the S/N ratio was set as the optimized condition because of the reduction of variance. Conditions C1 and D3 were set as the optimized ones.

3.4 Prediction and confirmation of the optimized conditions

(1) Prediction

The S/N ratio for the non-optimized conditions can be determined as

$$A1+B2+C2+D2+E2+F2+G2+H2-7T = 8.94 \text{ (dB)} \quad (1)$$

where A1 indicates the value of the S/N ratio for the first level of condition A. T indicates the mean. The S/N ratio of the optimized conditions can be determined as

$$A2+B3+C1+D3+E1+F1+G3+H2-7T = 27.29 \text{ (dB)} \quad (2)$$

The difference in the S/N ratio between the non-optimized and optimized conditions is more than 18 dB. It is expected that the variance can be reduced to less than 1/70 when optimized conditions are applied.

(2) Confirmation

To confirm the effects of welding and cooling conditions on the tensile residual stresses on the welded side of a specimen, three conditions were examined, as shown in Table 3: Condition A, welding with no water-shower cooling; condition B, welding in non-optimized conditions; and condition C, welding in the optimized conditions. The test specimens were Type 304 stainless-steel plates. The geometry of the test specimens is shown in Figure 9. The specimen size was 300 x 160 x 30 mm. Strain gauges were installed at the positions shown in Figure 9 to measure the residual stress.

Residual stress distributions along the transverse line in the welding-start, -steady, and -stop regions are shown in Figures 10, 11, and 12. Figure 10 shows the measured residual stress distributions when water-shower cooling was not applied. There is tensile stress in the longitudinal component whose value is more than 200 MPa. Figure 11 shows the measured residual stress distributions for the non-optimized condition. Some measured data indicate tensile stress. Figure 12 shows the measured residual stress distributions for the optimized condition. All of the residual stresses measured in the bead, fusion line, and HAZ became compressive.

To evaluate the effects of the conditions on residual stress distributions, the S/N ratio and sensitivity were calculated for these cases. Comparison of the S/N ratios between the non-optimized and the optimized conditions are shown in Table 4. The estimated improvement of the S/N ratio is 13.58 dB. On the other hand, the experimental value is 8.59 dB. The improvement indicates the variance can be

decreased to less than 1/10. The improvement of sensitivity in the analysis and the experiment also shows good agreement.

4. Verification of the effects of the interpass temperature on residual stress

In the prediction of optimized conditions using the robust design technique, we found that the effects of the interpass temperature on the S/N ratio and sensitivity are bigger than that of the other controllable parameters. Here, the relationship between the interpass temperature, which specially affects the S/N ratio and the sensitivity, and the mechanism of the tensile residual stress reduction is examined.

First, the residual stress distribution is calculated as a parameter of the interpass temperature using 3D-FEM. Second, the residual stress is measured in experiments. Then, the numerically calculated and experimentally measured residual stress data are compared to verify the accuracy of the analysis. Temperature distributions in the cross section of the plates are also studied to examine the relationship between the interpass temperature and the tensile residual stress reduction.

4.1 Conditions of analyses and experiments

The geometry of the specimen examined here is the same as the one examined in the previous section. The conditions of water-shower cooling and interpass temperature are shown in Table 5. The effects of water-shower cooling on residual stress are examined with or without the water-shower cooling. The effects of the interpass temperature on residual stress are also examined at interpass temperatures of 20, 100, and 200 °C.

A three-dimensional analysis model was used to calculate the temperature and residual stress distributions. Since the specimen is symmetrical, only half of the plate was analyzed. The residual stress distributions in the welded plate were evaluated in two steps using finite element analysis. First, the temperature distributions in the plate during welding and cooling were determined by a transient heat transfer analysis. Second, the results of the thermal analysis were used to estimate the residual stress distributions in the plate by a thermal-elasto-plastic analysis.

4.2 Analytical and experimental results

(1) Analytical results

Figures 13 and 14 show the contour lines of the residual stress derived from the theoretical analysis described in the previous section. These figures show the distribution of longitudinal stress and transverse stress.

Figure 13 shows the residual stress distribution after the plate is cooled in air. This figure shows that tensile stress remained on the surface and that its peak is more than 300 MPa. The longitudinal residual stress distribution in Figure 13 becomes tensile around the center of the welded region, and the residual stress becomes compressed away from the welded region. In addition, the residual-stress distribution along the centerline of the welding region was tensile from the welding start point to the stop point. In the transverse residual stress distribution in Figure 13, the stress along the centerline of the welded region is compressive from the welding starting point to the halfway point along the line. At the halfway point, it changed to tensile and remained so until the termination point. It can be concluded that the effects of preheating on residual stress were severely restricted in the case that the plate is cooled slowly in ambient air.

Figure 14 shows the residual stress distributions when the plate was cooled rapidly with a water-shower. This figure shows that residual stress was reduced to compressive on the surface and that it peaked at more than 100 MPa. Comparing the residual stresses on the surface shown in Figure 14 with that in Figure 13 shows that tensile residual stress at the surface of the plate is remarkably reduced by rapid cooling with a water shower.

When the welded plate was cooled slowly in air, the effect of preheating on the residual stress was restricted. On the other hand, when the welded plate was cooled rapidly with a water shower, tensile stress was reduced by a greater extent than without water-shower cooling.

(2) Comparison between analytical data and experimental data

Figure 15 compares the analytical and experimental longitudinal residual stress, and Figure 16 shows the transverse residual stress. These figures indicate that the residual stresses derived by analyzing the welded plate cooled slowly in air were tensile. These stresses are equivalent regardless of the application of preheating. When the welded plate was cooled slowly in air, the effect of preheating on the

residual stress was restricted. On the other hand, when the welded plate was cooled rapidly with a water-shower, the tensile stress was reduced by a greater extent than without water-shower cooling.

It can be concluded from the above results that the measured longitudinal residual stress and the transverse residual stress were tensile when the welded plate was cooled slowly in ambient air, and the effects of preheating on residual stress distributions were small. However, the tensile residual stress was reduced in the case of rapid cooling by a water-shower. In particular, the tensile residual stress transformed to compressive stress when rapid cooling followed preheating to 200 °C.

4.3 Temperature distributions in the welded plate

When the welded plate was cooled slowly in ambient air, tensile residual stress occurred in the welded region. The effect of the preheating on the residual stress distribution is severely restricted. On the other hand, when the welded plate was cooled rapidly by water-shower cooling, compressive residual stress occurs in the welded region. The effect of the preheating on the residual stress distribution is larger. Here, we examined the relationship between the residual stress distributions, the preheating temperature, and the cooling conditions from the view of the temperature distribution through the specimen, from the welded surface of the plate to the center of the welded metal.

Figure 17 shows the temperature distribution perpendicular to the surface at the center of the bead. Under ambient air conditions, the temperature at the surface rises to over 600 °C and gradually cools down perpendicular to the surface. The difference in the temperature between the surface and interior of the sample decreases 100 seconds after the torch passed at the point, before it finally reaches temperature of the ambient air.

Figure 18 shows the temperature distributions through the specimen from the welded surface of the plate when the plate was cooled rapidly by a water-shower with interpass temperatures of 20 and 200°C, respectively. In both cases, the temperature at the welded surface is lower than that in the interior of the plate. The temperature difference is 163 °C for an interpass temperature of 20 °C and 227 °C for an interpass temperature of 200 °C, respectively. The tendency of the temperature difference described here indicates that the higher the interpass temperature is set, the larger the temperature difference that occurs between the welded surface and the inside of

the plate. Tensile plastic strain is generated at the surface of the plate with these temperature distributions. As the temperature difference increases, the quantity of the plastic strain increases. The plastic strain causes compressive residual stress. As a result, high compressive residual stress is generated under the conditions of welding at high interpass temperatures and rapid cooling with a water-shower.

5. Conclusions

To reduce tensile residual stress on the surface of a structure after the last welding pass, a new welding method has been developed. In this method, a water-shower behind the welding torch cools the high temperature region on the welded surface. The welding and cooling conditions for reducing tensile residual stress were examined. A robust design technique was applied. The effects of the welding and rapid cooling conditions on the residual stress were evaluated quantitatively. Our conclusions are as follows.

(1) The optimized conditions to reduce tensile residual stress on the last-pass welded side are (a) one welding pass at the last layer, (b) a high interpass temperature, (c) low heat input quantity, (d) low travel speed, (e) a small distance between the torch and cooling area, (f) a wide cooling region, (g) a deep cooling region, and (h) a medium water-shower rate.

(2) The effect of the interpass temperature on the S/N ratio and the sensitivity is significantly larger than that of the other controllable parameters. The effect was verified by analyses and experiments.

Using the optimized conditions, compressive residual stress is generated on the last-pass welded surface at the welding-start point, welding-steady region, and welding-stop point. SCC does not occur under compressive stress. Therefore, it can be avoided by using the new welding method and the optimized conditions at welded regions of austenitic stainless steel.

References

[1] Ueda, Y., et al., 1986, Trans. ASME, J. Pres. Vessel Tech., Vol. 108, pp 14-23.

[2] Ueda, Y., et al., 1983, J. JWS, Vol. 52-2, pp 90-97. (in Japanese)

[3] Rybicki, E. F., et al., 1982, Trans. ASME, J. Eng. Mat. Tech., Vol. 104, pp 267-273.

[4] Shimizu, T., et al., 1987, Quar. J. JWS, Vol. 5-3, pp 49-55. (in Japanese)

[5] Sakata, S., et al., 1988, Quar. J. JWS, Vol. 6-1, pp 64-70. (in Japanese)

[6] White, R. A., et al., 1997, Welding J., Vol. 76, pp 57-61.

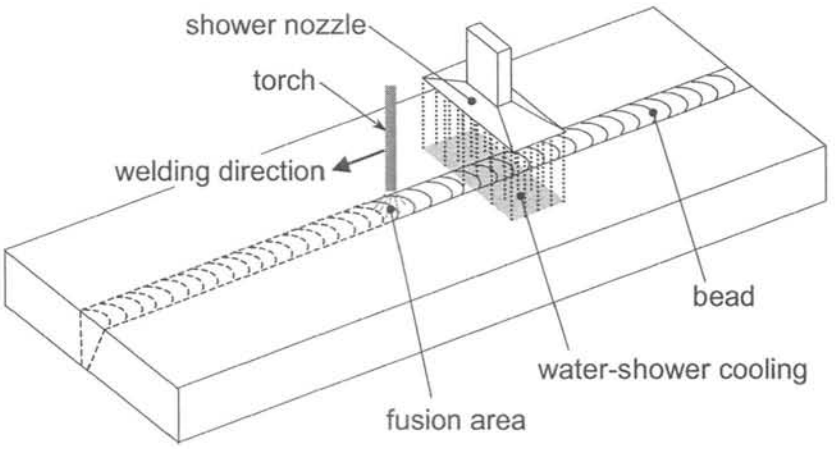

Fig. 1 Schematic of the new welding method

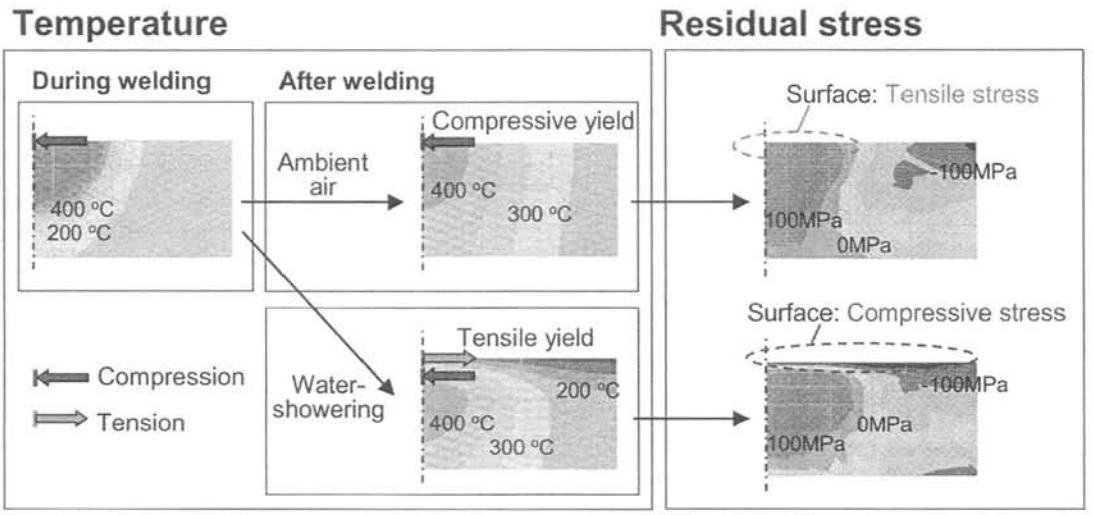

Fig. 2 Mechanism that produces residual stress

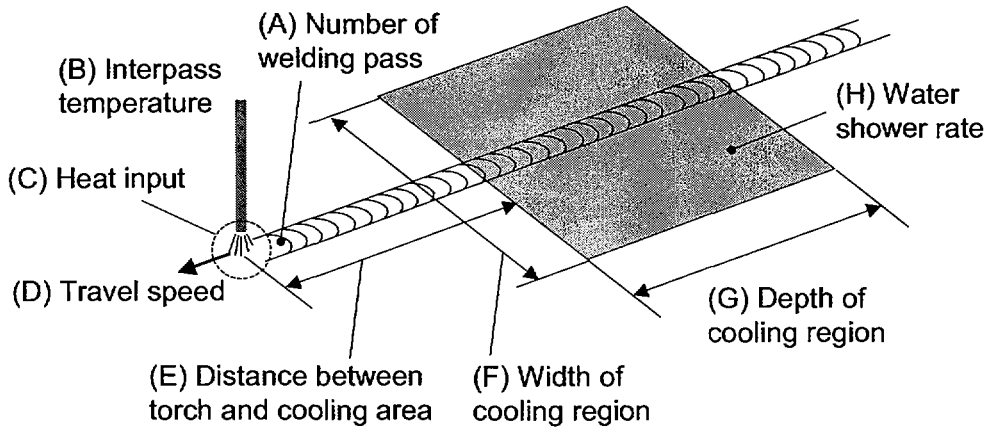

Fig. 3 Controllable parameters of new welding method

Table 1 Controllable parameters and their levels

Controllable parameter	Level 1	2	3
(A) Number of welding pass	**2**	**1**	**---**
(B) Interpass temperature	**Low**	**Medium**	**High**
(C) Heat input	**Low**	**Medium**	**High**
(D) Torch travel speed	**High**	**Medium**	**Low**
(E) Distance between torch and cooling	**Long**	**Medium**	**Short**
(F) Width of cooling region	**Long**	**Medium**	**(Long)**
(G) Depth of cooling region	**Short**	**Medium**	**Long**
(H) Water shower rate	**Low**	**Medium**	**High**

Table 2 L18 orthogonal array

Controllable parameter	Analytical condition No. 1	2	3	4	-----	16	17	18
(A)	**A1**	**A1**	**A1**	**A1**	**-----**	**A2**	**A2**	**A2**
(B)	**B1**	**B1**	**B1**	**B2**	**-----**	**B3**	**B3**	**B3**
(C)	**C1**	**C2**	**C3**	**C1**	**-----**	**C1**	**C2**	**C3**
(D)	**D1**	**D2**	**D3**	**D1**	**-----**	**D3**	**D1**	**D2**
(E)	**E1**	**E2**	**E3**	**E2**	**-----**	**E2**	**E3**	**E1**
(F)	**F1**	**F2**	**F3**	**F2**	**-----**	**F3**	**F1**	**F2**
(G)	**G1**	**G2**	**G3**	**G3**	**-----**	**G1**	**G2**	**G3**
(H)	**H1**	**H2**	**H3**	**H3**	**-----**	**H2**	**H3**	**H1**

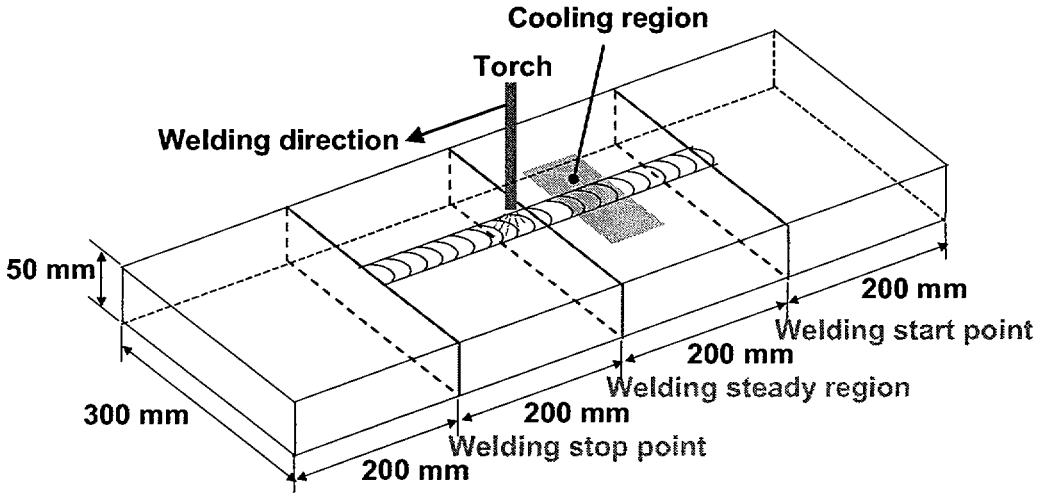

Fig. 4 Analytical model

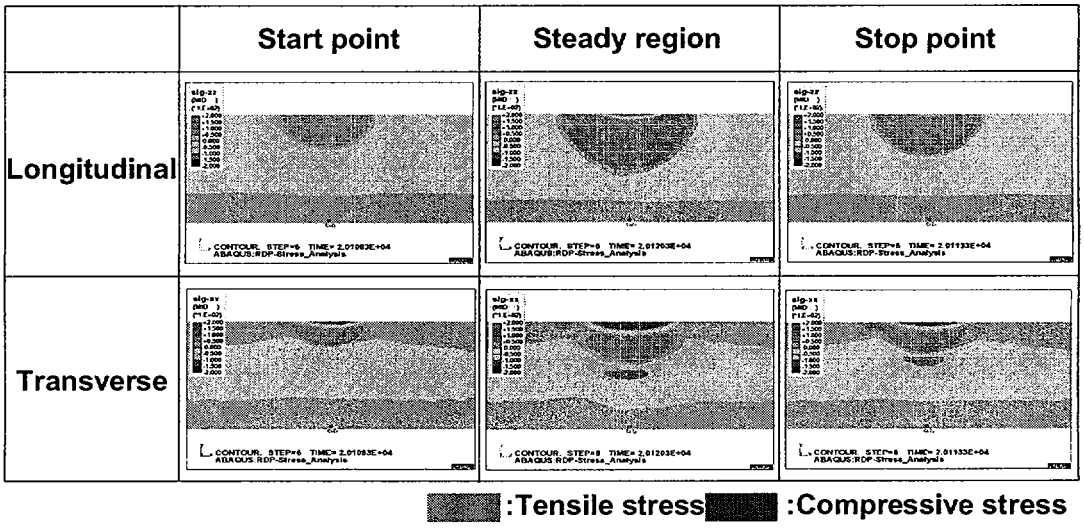

Fig. 5 Contour lines of residual stress in analytical condition No. 1

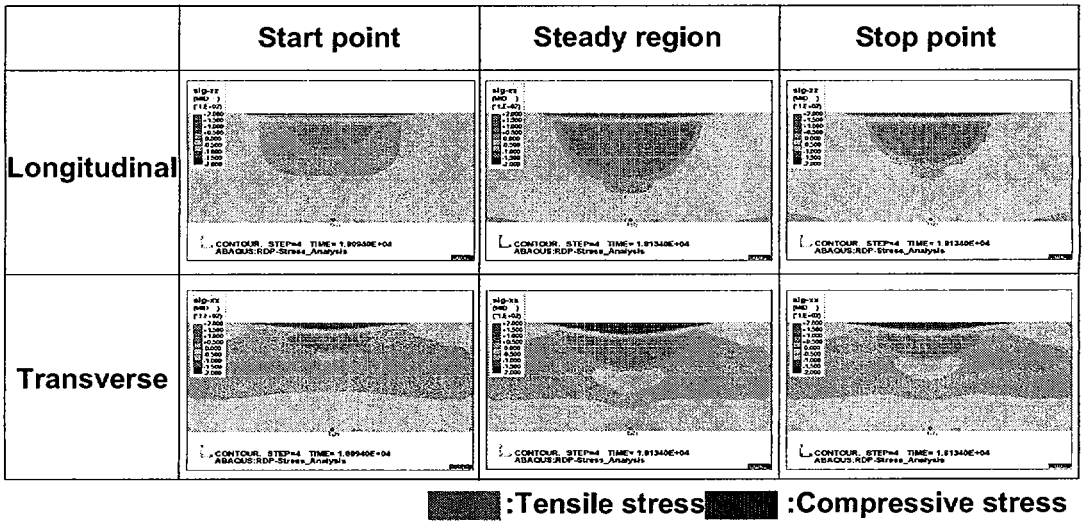

Fig. 6 Contour lines of residual stress in analytical condition No. 16

Analytical condition No.			Residual stress (MPa)								
			Start			Steady			Stop		
			Bead	FL	HAZ	Bead	FL	HAZ	Bead	FL	HAZ
1	L	N1	111	197	4	60	202	199	78	209	42
		N2	168	267	7	85	237	217	131	291	44
	T	N1	-196	110	84	-236	-101	198	-224	53	115
		N2	-142	195	92	-219	-49	223	-181	113	130
⋮ 18	⋮	⋮	⋮	⋮	⋮	⋮	⋮	⋮	⋮	⋮	⋮

Data analysis

L: Longitudinal
T: Transverse
FL: Fusion Line

Controllable parameter	S/N ratio (dB)			Sensitivity (dB)		
	1	2	3	1	2	3
(A)	10.61	12.97	---	51.20	52.18	---
(B)	4.85	10.26	20.27	49.01	52.12	53.95
⋮	⋮	⋮	⋮	⋮	⋮	⋮
(H)						

Fig. 7 Data analysis flow

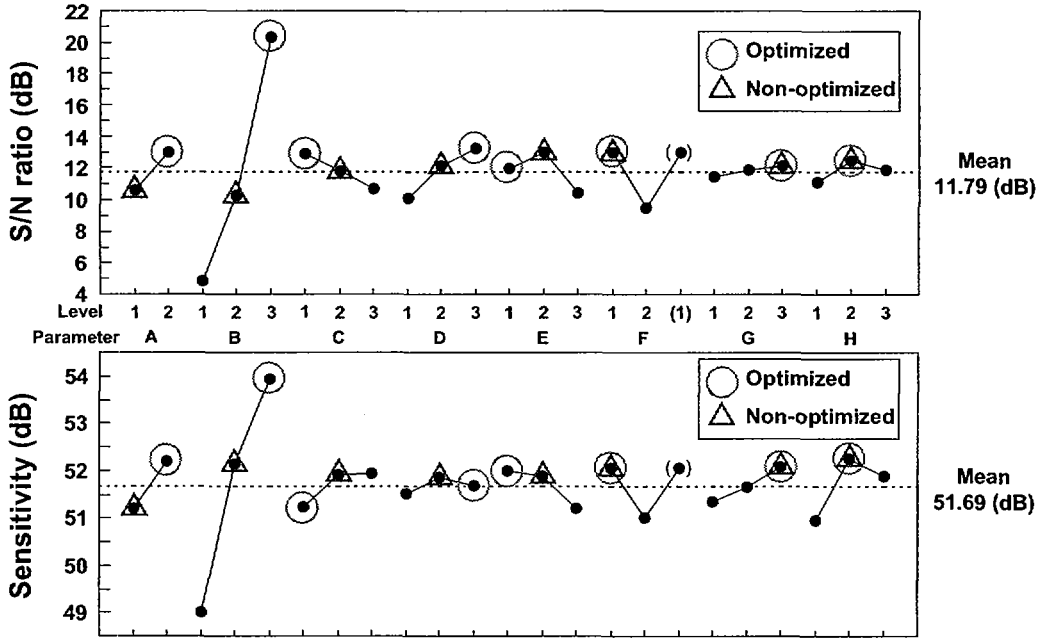

Fig. 8 Map of factor effects

Table 3 Experimental conditions for confirmation

Conditions / Controllable parameter	A without cooling	B non-optimized	C optimized
(A) Number of welding pass	1 (A2)	2 (A1)	1 (A2)
(B) Interpass temperature (°C)	200 (B3)	100 (B2)	200 (B3)
(C) Heat input (kJ/cm)	20 (C1)	30 (C2)	20 (C1)
(D) Torch travel speed (mm/min)	50 (D3)	90 (D2)	50 (D3)
(E) Distance between T and S (mm)	-----	50 (E2)	20 (E1)
(F) Width of cooling region (mm)	-----	80 (F1)	80 (F1)
(G) Depth of cooling region (mm)	-----	80 (G3)	80 (G3)
(H) Water shower rate (l/min)	-----	1 (H2)	1 (H2)

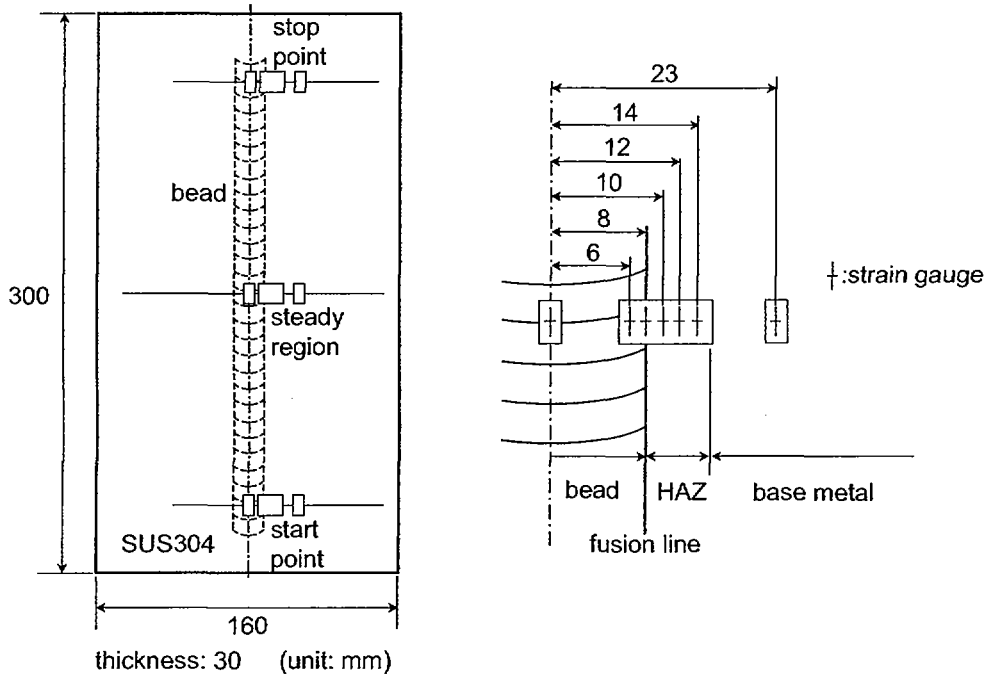

Fig. 9 Geometry of specimen

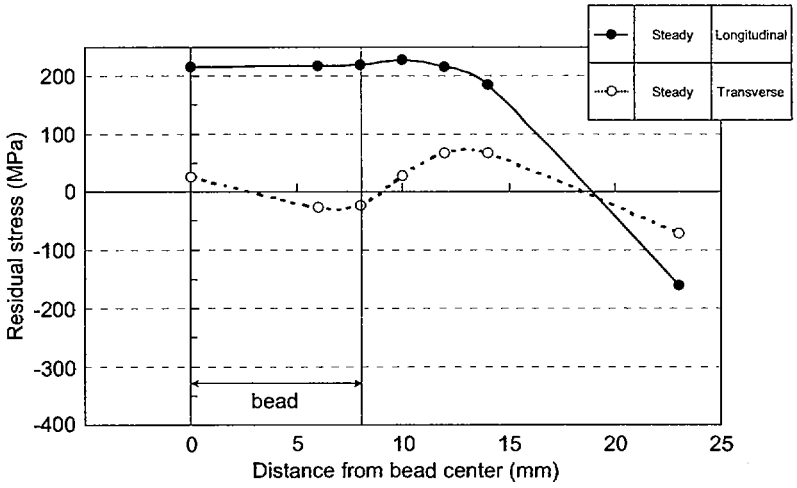

Fig. 10 Residual stress distributions in condition A

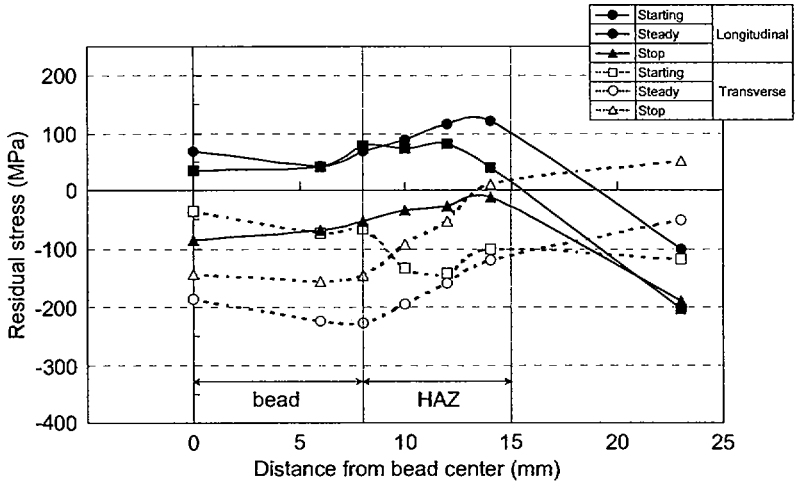

Fig. 11 Residual stress distributions in condition B (non-optimized)

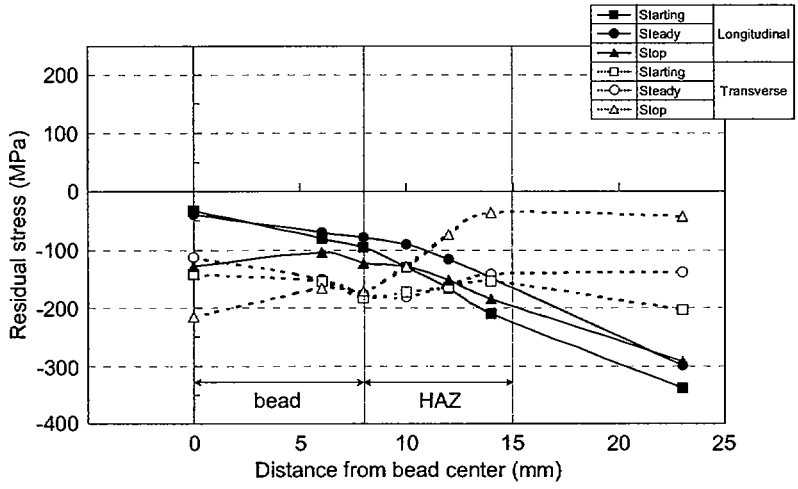

Fig. 12 Residual stress distributions in condition C (optimized)

Table 4 Comparison between analysis and experimental results

Character-istic / Conditions	S/N ratio (dB)		Sensitivity (dB)	
	Estimation	Experiment	Estimation	Experiment
Optimized	26.26	19.24	55.56	52.71
Non-optimized	12.68	10.65	53.51	50.77
Improvement	13.58	8.59	2.05	1.94

Table 5 Analytical and experimental conditions for verification

Conditions / Controllable parameter	1	2	3	4	5	6
(A):Number of welding pass	1	1	1	1	1	1
(B):Interpass temperature (°C)	20	100	200	20	100	200
(C):Heat input (kJ/cm)	20	20	20	20	20	20
(D):Torch travel speed (mm/min)	50	50	50	50	50	50
(E):Distance between torch and shower (mm)	Without water-shower cooling			20	20	20
(F):Width of cooling region (mm)				80	80	80
(G):Depth of cooling region (mm)				80	80	80
(H):Water supply rate (l/min)				1	1	1

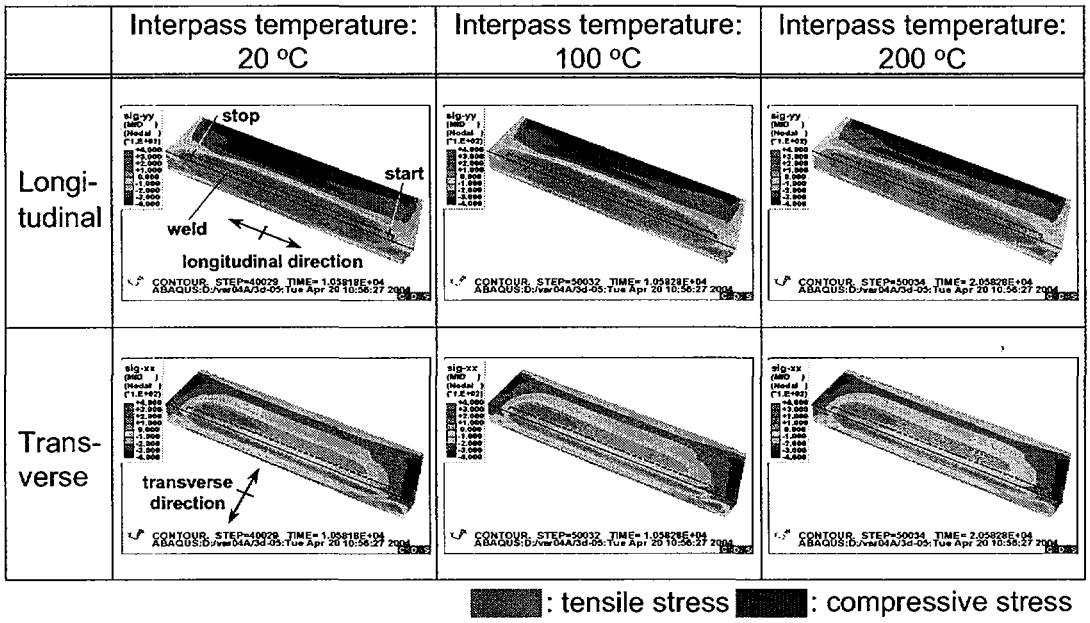

Fig. 13 Residual stress distribution for ambient-air cooling

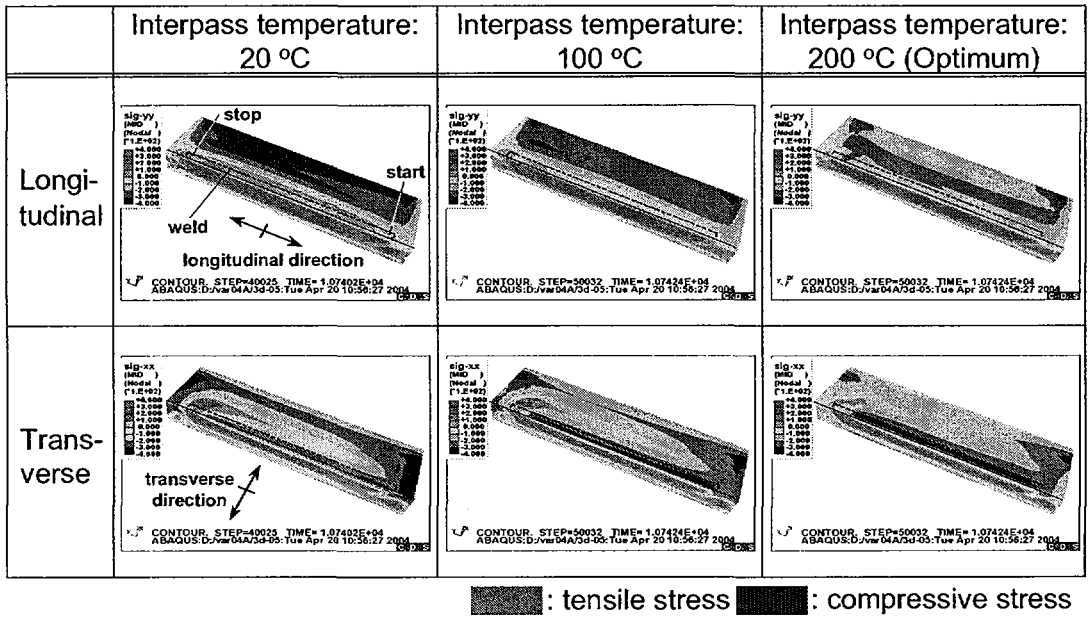

Fig. 14 Residual stress distribution for water-shower cooling

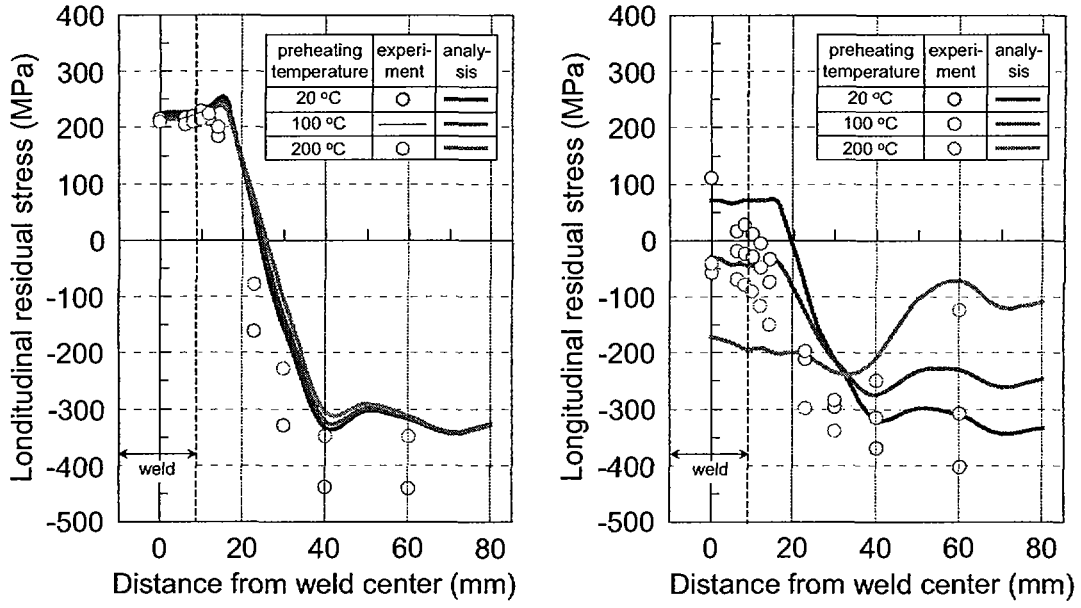

(a) Ambient-air cooling (b) Water-shower cooling

Fig. 15 Longitudinal residual stress distribution

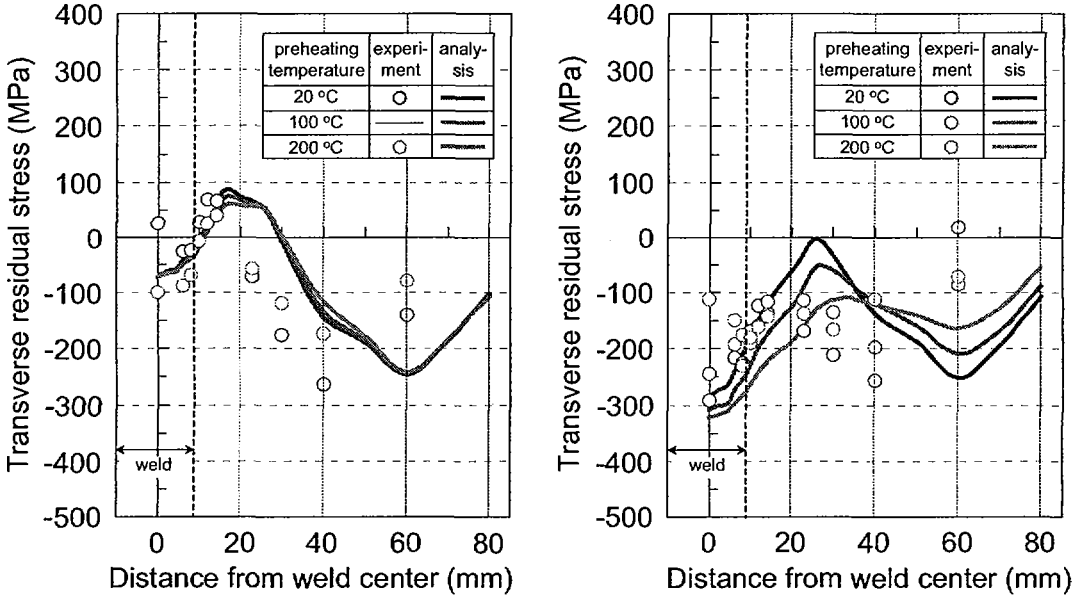

(a) Ambient-air cooling (b) Water-shower cooling

Fig. 16 Transverse residual stress distribution

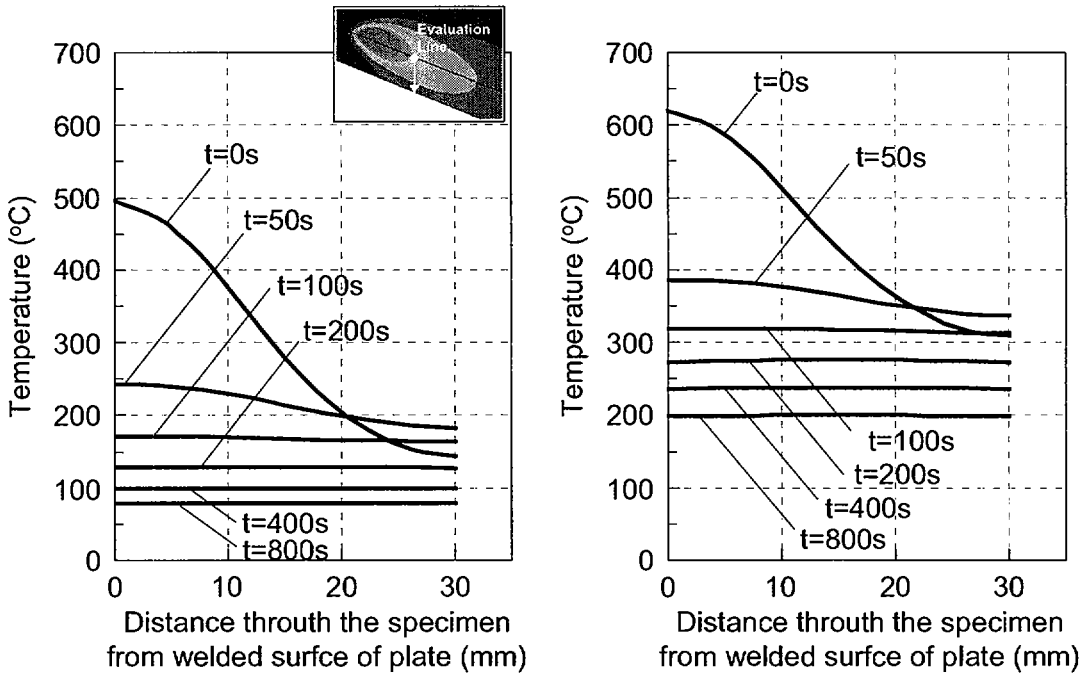

(a) Interpass temperature 20 °C (b) Interpass temperature 200 °C

Fig. 17 Temperature distribution through the specimen from welded surface of plate cooled slowly in ambient air

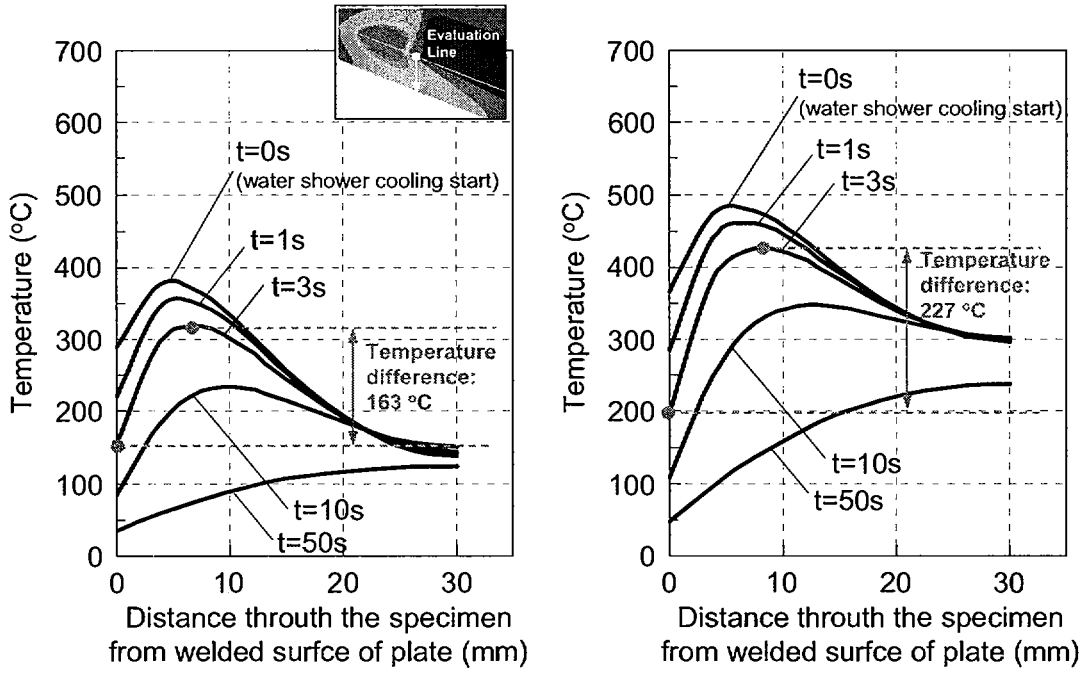

(a) Interpass temperature 20 °C (b) Interpass temperature 200 °C

Fig. 18 Temperature distribution through the specimen from welded surface of plate cooled rapidly by water-shower cooling